

New limits on spin-independent couplings of low-mass WIMP dark matter with a germanium detector at a threshold of 200 eV

S.T. Lin,¹ H.B. Li,¹ X. Li,² S.K. Lin,¹ H.T. Wong,^{1,*} M. Deniz,^{1,3} B.B. Fang,² D. He,² J. Li,^{2,4} C.W. Lin,¹
F.K. Lin,¹ V. Singh,¹ X.C. Ruan,⁵ J.J. Wang,¹ Y.R. Wang,¹ S.C. Wu,¹ Q. Yue,² and Z.Y. Zhou⁵

(TEXONO Collaboration)

¹ *Institute of Physics, Academia Sinica, Taipei 115, Taiwan.*

² *Department of Engineering Physics, Tsinghua University, Beijing 100084, China.*

³ *Department of Physics, Middle East Technical University, Ankara 06531, Turkey.*

⁴ *Institute of High Energy Physics, Chinese Academy of Science, Beijing 100039, China.*

⁵ *Department of Nuclear Physics, Institute of Atomic Energy, Beijing 102413, China.*

(Dated: February 6, 2020)

An energy threshold of 200 eV was achieved with a four-channel ultra-low-energy germanium detector each with an active mass of 5 g. This low threshold provides unique probe to WIMP dark matter with mass below 10 GeV. Using 0.338 kg-day of low-background data taken at the Kuo-Sheng Reactor Laboratory, constraints on WIMPs in the galactic halo were derived. The limits improve over previous results on the spin-independent couplings with the nucleons for WIMP mass between 3–6 GeV. Sensitivities for full-scale experiments were projected. This detector technique makes the unexplored sub-keV energy window accessible for new neutrino and dark matter experiments.

PACS numbers: 95.35.+d, 29.40.-n, 98.70.Vc

There are compelling evidence from cosmological and astrophysical observations that about one quarter of the energy density of the universe is due to Cold Dark Matter (CDM), whose nature and properties are still unknown [1]. Weakly Interacting Massive Particles (WIMP, denoted by χ) are the leading candidates for CDM. There are intense experimental efforts [2] to look for WIMPs through direct detection of nuclear recoils in $\chi N \rightarrow \chi N$ elastic scattering or in the studies of the possible products through $\chi\bar{\chi}$ annihilations.

Supersymmetric (SUSY) particles [3] are the leading WIMP candidates. The popular SUSY models prefer WIMP mass (m_χ) of the range of ~ 100 GeV, though light neutralinos remain a possibility [4]. Most experimental programs optimize their design in the high-mass region and exhibit diminishing sensitivities for $m_\chi < 10$ GeV, where there is an allowed region if the annual modulation data of the DAMA experiment [5] are interpreted as WIMP signatures. Simple extensions of the Standard Model with a singlet scalar favors light WIMPs [6]. To probe the low-mass region, detector with sub-keV threshold is necessary. Such threshold will also allow the studies of WIMPs bound in the solar system [7], and non-pointlike SUSY candidates like Q-balls [8]. Sensitivity to sub-keV energy presents a formidable challenge to detector technology and to background control. Only the CRESST-I experiment has derived exclusion limits [9] with sapphire(Al_2O_3)-based cryogenic detector at a threshold of 600 eV.

A research program in low energy neutrino and astroparticle physics is being pursued at the Kuo-Sheng(KS) Reactor Laboratory [10]. A scientific goal is to develop advanced detectors with kg-size target mass, 100 eV-range threshold and low-background spec-

ifications for WIMP searches as well as the studies of neutrino-nucleus coherent scattering [11] and neutrino magnetic moments (μ_ν) [12]. The KS laboratory is located 28 m from a 2.9 GW reactor core and has an overburden of about 30 meter-water-equivalent. Its facilities were described in Ref. [13], where μ_ν -limits with a 1.06 kg germanium detector (HPGe) at a hardware threshold of 5 keV were reported. These data were also used in the studies of reactor electron neutrinos [14] and for reactor axions searches [15]. The experimental procedures were well-established and the background were measured. In particular, a background level of ~ 1 event $\text{kg}^{-1}\text{keV}^{-1}\text{day}^{-1}$ (cpd) at 20 keV, comparable to those of underground CDM experiments, was achieved.

Ultra-low-energy germanium detectors (ULEGe) is a matured technique and are used in the measurements of soft X-rays. These detectors typically have modular mass of 5 – 10 g while detector array of up to 30 elements have been constructed. This technology was adopted to explore the sub-keV regime. Compared to Al_2O_3 , Ge provides enhancement in the χN spin-independent couplings ($\sigma_{\chi N}^{\text{SI}}$) due to the A^2 dependence [1, 16], A being the mass number of the target isotopes. Spin-dependent couplings, however, are suppressed by the low isotopic abundance (7.8%) of ^{73}Ge in natural germanium. For detectors like the ULEGe, only $\sim 20\%$ of the nuclear recoil energy due to χN interactions would give rise to observable ionization energy. The suppression ratio is called the quenching factor (QF) [17]. The energy dependence of QF in Ge was evaluated with the TRIM software package [18]. The results were in good agreement with available data [19], especially in the 1–10 keV recoil energy range relevant to the present analysis.

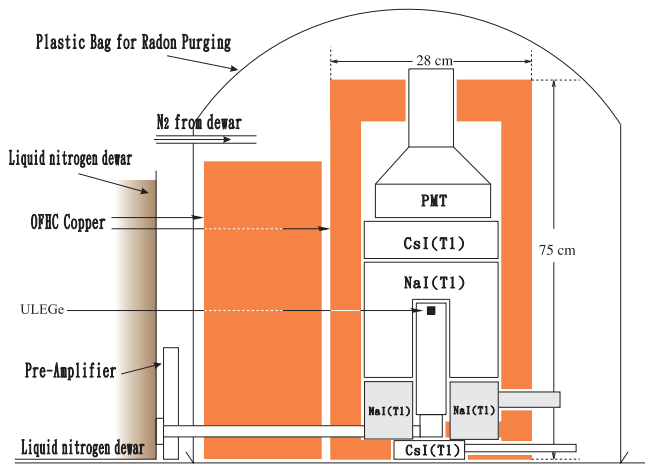


FIG. 1: Schematic layout of the ULEGe with its anti-Compton detectors as well as inner shieldings and radon purge system. Enclosing the system is a 50-ton shielding and cosmic-ray veto structures [13] which are not shown.

Results reported in this article were derived from data taken at KS with a 4-element ULEGe array, each having an active mass of 5 g [20]. Standard ultra-low-background specifications were adopted in its construction and choice of materials. It has the same external dimensions as the 1-kg HPGe of Ref. [13]. Apart from replacing with the ULEGe, data taking was performed with the anti-Compton (ACV) and cosmic-ray veto (CRV) systems, shieldings configurations, electronics and data acquisition (DAQ) systems [21] kept identical. The schematic layout of experiment components inside the shieldings is depicted in Figure 1. Data taking was performed in conjunction with a CsI(Tl) scintillator array [22] for the studies of neutrino-electron scattering. The combined DAQ rate was about 30 Hz, and the DAQ dead time was accurately measured to be 11.0% using random trigger (RT) events uncorrelated with the rest of the system [13].

The ULEGe signals were provided by built-in pulsed optical feedback pre-amplifiers, and were distributed to two spectroscopy amplifiers at 6 μ s (SA_6) and 12 μ s (SA_{12}) shaping times and different amplification factors. Discriminator output of SA_6 provided the trigger definitions for DAQ. At a threshold setting of 20 eV energy equivalence, the DAQ rates for the ULEGe system were about 5 Hz due mostly to electronic noise. The SA_6 , SA_{12} , ACV and CRV signals were read out by 20 MHz Flash Analog-to-Digital Convertors. Various system control parameters were also recorded. Taking the trigger instant as $t=0$, the energy of SA_6 and SA_{12} was defined by integrating the pulse within $(-20,52)$ μ s and a restricted interval of $(15,25)$ μ s, respectively.

Depicted in Figure 2a is an energy calibration spectrum due to external ^{55}Fe sources (5.90 and 6.49 keV) together with X-rays from Ti (4.51 and 4.93 keV),

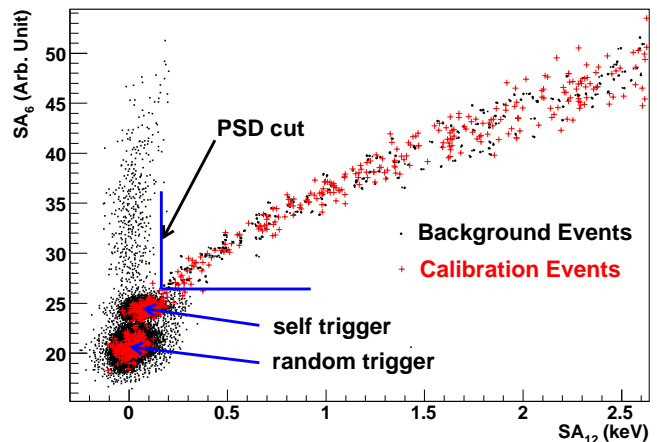
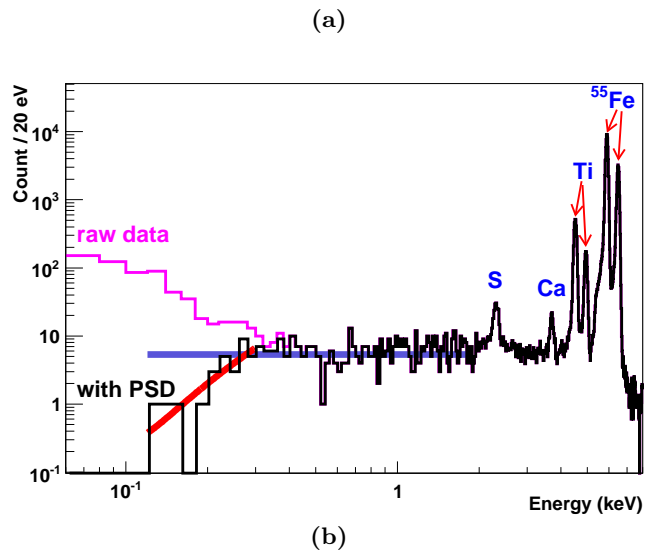


FIG. 2: (a) Measured energy spectrum of the ULEGe with ^{55}Fe source showing also X-ray peaks from various materials. The best-fit of the spectrum at 0.5 – 2 keV is extrapolated to low energy. The black histogram represents events selected by PSD cuts. Deviations from the expected spectra contribute to PSD efficiencies. (b) Scattered plots of the SA_{12} versus SA_6 signals, constrained by both energy and timing, for both calibration and physics events. The PSD selection is shown.

Ca (3.69 keV), and S (2.31 keV). Photons with lower energy than 2 keV were completely absorbed by the detector window. The RT-events provided the calibration point at zero-energy. The RMS resolutions for the RT-events and ^{55}Fe peaks were about 55 eV and 78 eV, respectively. The calibrations were performed before and after the DAQ periods. Linearity was checked up to 60 keV with various γ -sources, and between zero and 2 keV with a precision pulse generator. The energy scale was accurate to < 20 eV, while deviations from linearity were $< 1\%$. The system instabilities, also monitored in situ by the pulse generator, were $< 5\%$.

The analysis procedures followed closely to those of the μ_ν studies [13]. Events with CRV and ACV tags were re-

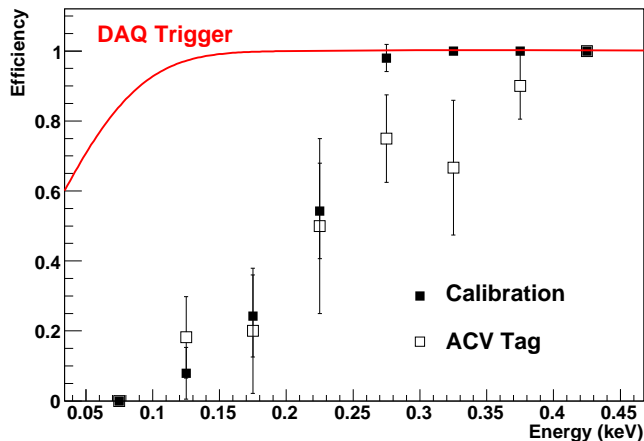


FIG. 3: Selection efficiencies of the PSD cut, as derived from the ^{55}Fe -source calibration and from in situ data with ACV tags. The solid line represents the trigger efficiency where physics events were recorded by the DAQ system.

jected. The surviving events were ULEGe signals uncorrelated with other detector systems and could be WIMP candidates. The spectrum of Figure 2a indicates a detector threshold or “noise-edge” of about 300 eV. Based on correlations on both the energy and timing information of the SA₆ and SA₁₂ signals, pulse shape discrimination (PSD) software was devised to differentiate physics events from those due to electronic noise. Displayed in Figure 2b is a scattered plot of the SA₆ and SA₁₂ signals, with the PSD cut superimposed. The noise events were suppressed. Calibration events and those from physics data taking were overlaid, indicating uniform response.

Studies on the survival efficiencies of the physics events were performed. The trigger efficiencies, displayed in Figure 3, were evaluated using as input the discriminator threshold of 20 eV and the measured RMS of 55 eV for RT-events. The efficiencies of the ACV and CRV cuts, as derived from RT-events [13], are 98.3% and 91.5%, respectively. The PSD selection efficiencies were evaluated by two independent methods. The physics events in the ^{55}Fe spectra of Figure 2a should give rise to a flat distribution down to low energy. The deviations of the PSD-selected events from a flat distribution provided an efficiency measurement. Alternatively, a pure sample of physics events was extracted from in situ data with ACV tags. The fraction of these events surviving the PSD cuts represented the selection efficiency. Consistent results from both approaches were obtained, as shown in Figure 3. A threshold of 200 eV was achieved at an efficiency of about 50%.

Data were taken with the ULEGe at KS under different hardware and software configurations. They provided important input on the background understanding and performance optimizations of this novel detector, both of which are essential for future full-scale experiments.

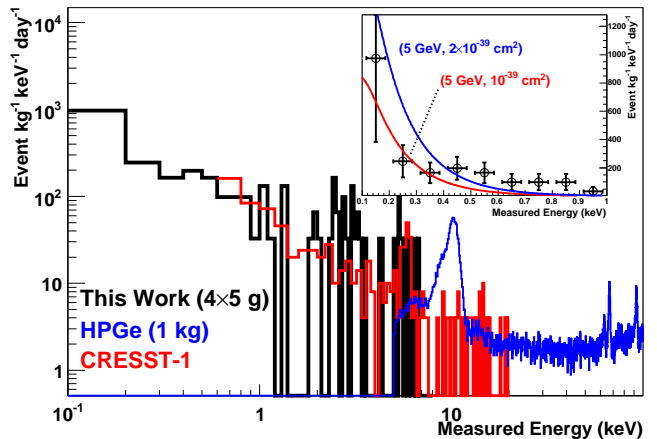


FIG. 4: The measured spectrum of ULEGe with 0.338 kg-day of data, after CRV, ACV and PSD selections. Background spectra of the CRESST-I experiment [9] and the HPGe [13] are overlaid for comparison. The expected nuclear recoil spectra for two cases of $(m_\chi, \sigma_{\chi N}^{\text{SI}})$ are superimposed onto the spectrum shown in linear scales in the inset.

Results of these studies will be published. The best background and threshold is from a configuration with 0.338 kg-day of data. The ULEGe spectrum normalized in cpd unit after the CRV, ACV and PSD selections is displayed in Figure 4, showing comparable background as CRESST-I [9]. The statistical uncertainties at threshold were about 50%, dominating over the systematic effects due to calibrations and stabilities.

Exclusion limits were derived from the spectrum of Figure 4 on the $(m_\chi, \sigma_{\chi N}^{\text{SI}})$ plane. The standard and conservative approach that the WIMP signals cannot be larger than the observed event rates was adopted. The formalisms followed those of Ref. [16] using standard nuclear form factors and a local WIMP density of 0.3 GeV cm^{-3} with Maxwellian velocity distribution. Corrections due to QF, detector resolution and different efficiency factors were incorporated. The optimal interval method as adopted by other CDM experiments [9, 23] was used. Possible energy intervals larger than 100 eV (twice the RMS resolution) were sampled. By comparing the observed background in those intervals to the expected number of events due to χN recoils for each m_χ , the optimal intervals producing the most stringent limits to $\sigma_{\chi N}^{\text{SI}}$ were selected. In practice, event rates at the 150-250 eV interval defined the sensitivities for $m_\chi < 10 \text{ GeV}$.

The exclusion plots of $\sigma_{\chi N}^{\text{SI}}$ versus m_χ at 90% confidence level for galactically-bound WIMPs are displayed in Figure 5. The allowed regions of DAMA [5] and the limits from experiments currently defining the exclusion boundaries [9, 24] are displayed. New limits were set by the KS-ULEGe data in $\sigma_{\chi N}^{\text{SI}}$ for $m_\chi \sim 3 - 6 \text{ GeV}$, the sensitivities enhanced mainly by the A^2 factor in $\sigma_{\chi N}^{\text{SI}}$. A portion of the DAMA region at low m_χ was probed and excluded. The observable nuclear recoils after QF

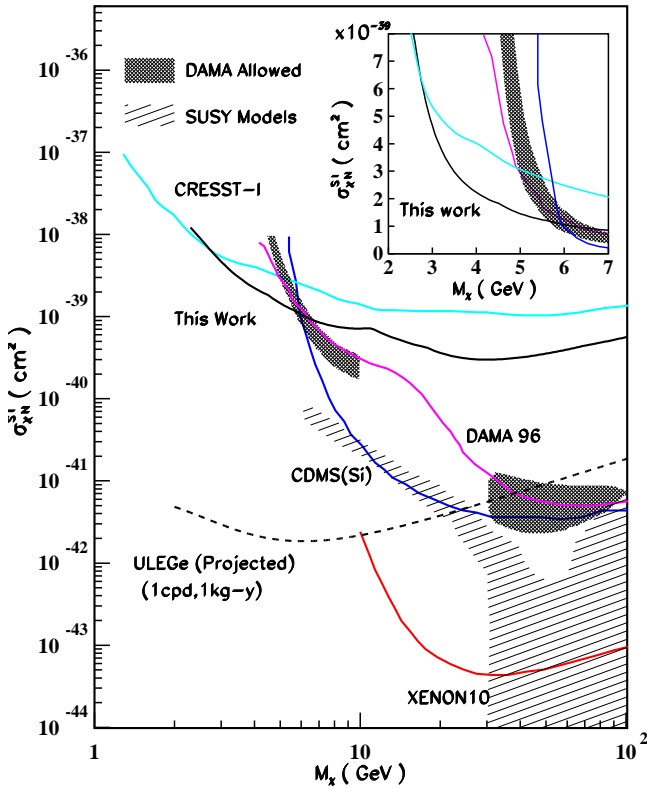


FIG. 5: Exclusion plots of spin-independent χN cross-section versus WIMP-mass, displaying the KS-ULEGe limits and those from various experiments defining the current boundaries [9, 24]. The DAMA allowed regions [5] are superimposed. The striped region is that favored by SUSY models [4]. Projected sensitivities of full-scale experiments are indicated as dotted lines. The relevant region is presented with linear scales in the inset.

corrections at $m_\chi=5$ GeV and $\sigma_{\chi N}^{SI}=10^{-39}$ cm² (allowed) and 2×10^{-39} cm² (excluded) are superimposed with the measured spectrum in Figure 4.

This work improves the bounds on WIMP at the less-explored m_χ range by making measurements at a new observable window of 100 eV–1 keV in a low-background environment. Understanding and suppression of background at this sub-keV region is crucial for further improvement on the sensitivities. Measurements are conducted with the ULEGe at an underground laboratory. There are recent important advances in a new design in ULEGe [25] which offer great potentials of scaling-up the detector mass to the kg-range. The mass-normalized external background will be reduced in massive detectors due to self-attenuation [11]. The potential reach of full-scale experiments with 1 kg-year of data strength and background level of 1 cpd is illustrated in Figure 5. Such experimental programs are complementary to the many current efforts on CDM direct searches.

The authors are grateful to inspiring discussions with

Prof. S.K. Kim and the KIMS Collaboration. This work is supported by the Academia Sinica Pilot Project Funds 2004-06, as well as contracts 95-2119-M-001-028 and 96-2119-M-001-005 from the National Science Council, Taiwan and 10620140100 from the National Natural Science Foundation, China.

* Corresponding Author: htwong@phys.sinica.edu.tw; Tel:+886-2-2789-9682; FAX:+886-2-2788-9828.

- [1] M. Drees and G. Gerbier, *J. Phys. G* **33**, 233 (2006), and references therein.
- [2] R.J. Gaitskell, *Annu. Rev. Nucl. Part. Sci.*, **54**, 315 (2004), and references therein.
- [3] H. H. Haber and M. Schmitt, *J. Phys. G* **33**, 1105 (2006), and references therein.
- [4] A. Bottino et al., *Phys. Rev. D* **72**, 083521 (2005).
- [5] C. Savage, P. Gondolo and K. Freese, *Phys. Rev. D* **70**, 123513 (2004); P. Gondolo and G. Gelmini, *Phys. Rev. D* **71**, 123520 (2005).
- [6] X.G. He et al., *Mod. Phys. Lett. A* **22**, 2121 (2007).
- [7] T. Damour and L.M. Krauss, *Phys. Rev. Lett.* **81**, 5726 (1998); J.I. Collar, *Phys. Rev. D* **59**, 063514 (1999).
- [8] G. Gelmini, A. Kusenko and S. Nussinov, *Phys. Rev. Lett.* **89**, 101302 (2002).
- [9] G. Angloher et al., *Astropart. Phys.* **18**, 43 (2002).
- [10] H.T. Wong, *Mod. Phys. Lett. A* **19**, 1207 (2004).
- [11] H.T. Wong et al., *J. Phys. Conf. Ser.* **39**, 266 (2006).
- [12] H.T. Wong and H.B. Li, *Mod. Phys. Lett. A* **20**, 1103 (2005).
- [13] H.B. Li et al., *Phys. Rev. Lett.* **90**, 131802 (2003); H.T. Wong et al., *Phys. Rev. D* **75**, 012001 (2007).
- [14] B. Xin et al., *Phys. Rev. D* **72**, 012006 (2005).
- [15] H.M. Chang et al., *Phys. Rev. D* **75**, 052004 (2007).
- [16] J.D. Lewin and P.F. Smith, *Astropart. Phys.* **6**, 87 (1996).
- [17] J. Lindhard et al., *Dan. Vid. Mat.-Fys. Medd.* **33**, 10 (1963); J.F. Ziegler, J.P. Biersack and U. Littmark, *The Stopping and Range of Ions in Solid*, Pergamon Press (1985).
- [18] J.F. Ziegler, *Transport of Ions in Matter*, <http://www.srim.org> (1998).
- [19] K.W. Jones and H.W. Kraner, *Phys. Rev. C* **1**, 125 (1971); K.W. Jones and H.W. Kraner, *Phys. Rev. A* **11**, 1347 (1975); T. Shutt et al., *Phys. Rev. Lett.* **69**, 3425 (1992); Y. Messous et al., *Astropart. Phys.* **3**, 361 (1995).
- [20] Manufacturer: Canberra Industries, Inc.
- [21] W.P. Lai et al., *Nucl. Instrum. Methods A* **465**, 550 (2001).
- [22] H.B. Li et al., *Nucl. Instrum. Methods A* **459**, 93 (2001).
- [23] A. de Bellefon et al., *Astropart. Phys.* **6**, 35 (1996); L. Baudis et al., *Phys. Rev. D* **59**, 022001 (1998); A. Morales et al., *Phys. Lett. B* **489**, 268 (2000); S. Cebrian et al., *Astropart. Phys.* **15**, 79 (2001).
- [24] R. Bernabei et al., *Phys. Lett. B* **389**, 757 (1996); D.S. Akerib et al., *Phys. Rev. Lett.* **96**, 011302 (2006); J. Angle et al., arXiv:astro-ph/0706.0039 (2007).
- [25] P.A. Barbeau, J.I. Collar and O. Tench, *JCAP* **09**, 009 (2007).